

THE 4TH INTERNATIONAL CONFERENCE ON ALUMINUM ALLOYS

PREDICTION OF SMALL CRACK GROWTH FROM BULK FATIGUE BEHAVIOUR

Xu Dong Li and Lyndon Edwards

Fracture Research Group, Materials Discipline, Faculty of Technology, The Open University,
Milton Keynes, MK7 6AA, UK

Abstract

The fatigue behaviour of 7150-T651 aluminium alloy has been studied using both strain-controlled low cycle fatigue tests and stress-controlled four point bend tests in order to see if small fatigue crack growth can be related to bulk fatigue properties measured from smooth specimens. Using these results a model has been developed that uses the concept of a process zone to represent the fully damaged zone ahead of a small crack tip. Using this damage mechanics methodology, quantitative predictions of small crack growth rates have been made that rely only on appropriate physical description of the alloy through its bulk materials properties in conjunction with microstructural characteristics.

Introduction

Fatigue design of components in many industries is still based on the use of S-N curves which although based on total life, essentially represent design against crack initiation since the major portion of the lifetime is spent in the formation of an engineering-size crack. However, we now know that cracks initiate on a microstructural size scale much earlier than this and the majority of the fatigue life is spent in small crack growth. Thus, a number of workers have developed defect-tolerant approaches to fatigue life prediction by modelling small fatigue crack growth, (1-3). The fatigue lifetime is then assessed in terms of the number of cycles to propagate the largest crack-like defect to failure. Although these models are scientifically elegant, their application to fatigue life prediction requires the determination of an expression for crack growth, which is obtained from careful and tedious characterisation of small fatigue cracks. This limits the general applicability of such models as the acquisition of such data is expensive and standards for both material property definition and measurement have yet to be agreed. This paper describes initial attempts to model small fatigue crack growth using only bulk fatigue properties and knowledge of the microstructural features.

Materials and Methods

The alloy studied was a conventionally-cast ingot metallurgy aluminium alloy, 7150-T651 supplied by Alcan Int. Ltd. Its nominal chemical composition was Si=0.07%, Fe=0.11%, Cu=2.10%, Mg=2.16, Zn=6.16%, Ti=0.02%, Zr=0.13%, Al=balance and it has a yield stress of 421MPa, a tensile strength, of 600MPa and an average grain size of 18 μm . Fully reversed, strain-controlled, tension-compression ($R=-1$) low-cycle fatigue tests were performed using smooth cylindrical specimens at a constant strain rate of $1 \times 10^{-3} \text{ s}^{-1}$ to measure the bulk fatigue properties of the material. Small fatigue crack growth was characterised using a surface replica technique on unnotched four-point bend specimens at a load ratio R of 0.1.

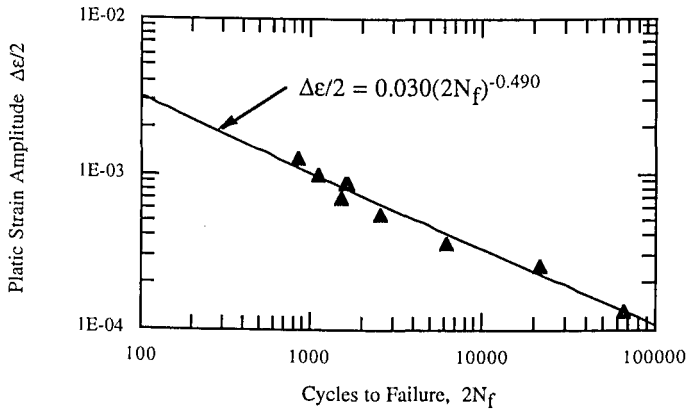


Figure 1 Strain Life Curves

Results

The results of the strain-controlled low cycle fatigue tests are shown in Figure 1. This curve is well characterised by the well known Coffin-Manson relation:

$$\frac{\Delta \epsilon}{2} = \frac{\sigma'_f}{E} (2N_f)^b + \epsilon'_f (2N_f)^c \quad (1)$$

where for this alloy $\sigma'_f=1199\text{MPa}$, $b=-0.108$, $\epsilon'_f=0.03$ and $c=-0.49$.

Figure 2 shows typical cyclic stress response curves. Cyclic softening behaviour is evident throughout all strain ranges and is preceded by detectable cyclic hardening only at the lowest applied strain value. Furthermore the degree of cyclic softening increases with applied strain amplitude. This behaviour is typical of peak aged aluminium alloys, (4). Cyclic softening occurs due to shearing of the ageing precipitates during cyclic straining which causes inhomogeneous slip and consequent strain localisation.

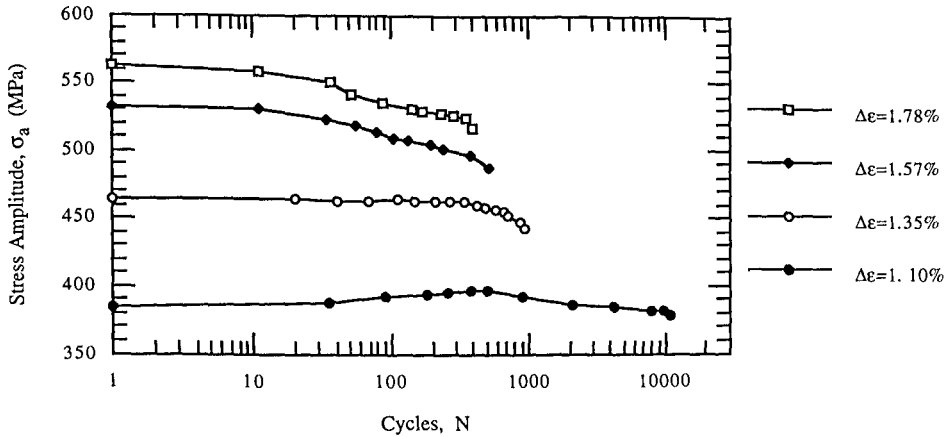


Figure 3 Cyclic Stress-Strain Response Curves

With increasing applied strain both the number of slip bands and the number of dislocations in each band increases leading to a higher flow stress due to work hardening. The kinetics of cyclic softening are dependent on the rate of dislocation cutting of the ageing precipitate and hence on the number of mobile dislocations in a given slip band. As the number of mobile dislocations in the slipband increases with strain then the rate of cyclic softening is greater at higher applied strains. The cyclic stress-strain curve for the alloy, (Figure 3), was measured using a multiple step test. The curve is well approximated by the equation:

$$\frac{\Delta \epsilon_p}{2} = \left(\frac{\Delta \sigma}{2K'} \right)^{\frac{1}{n'}} \quad (2)$$

where for this alloy, $K' = 814.2 \text{ MPa}$, and $n' = 0.0712$.

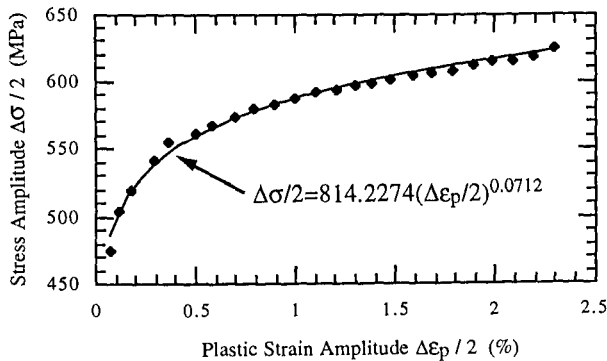


Figure 4 Cyclic Stress Strain Curve

The Model

Since small fatigue crack propagation is heavily affected by material microstructure and in particular by crystal misorientation at grain boundaries it is necessary to relate the stress-strain field just ahead of a small fatigue crack tip in terms of appropriate microstructural dimensions. Using an approach similar to Forsyth, (5) we conceive the material to be composed of elementary blocks of finite linear dimension, ρ^* , ahead of the crack tip. At its simplest each elementary block can be considered to be one grain. However, other material characteristics such as grain orientation, surface texture, or interphase stresses can also be seen to contribute to properties of the material in each microstructural dimension, ρ^* . Of course, the stress/strain distribution varies throughout a cracked grain so uniform stress/strain conditions are assumed to only occur within a 'process zone' just ahead of the crack tip of size, d^* . To simplify the model we assume that the small crack and its associated slip bands are coplanar and that the slip bands do not initially impinge on the grain boundary. This agrees with previous observations on the plasticity associated with small fatigue cracks in 7000 series aluminium alloys, (6,7). A schematic representation of the model is given in Figure 4.

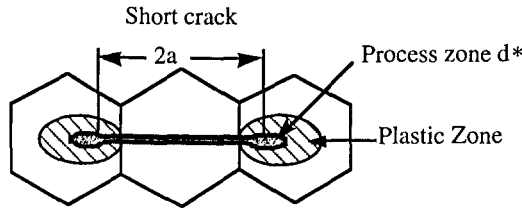


Figure 4 The Small fatigue Crack Model

It is the accumulation of fatigue damage over this process zone that controls crack propagation. So the crack growth rate at any time will be given by the process zone size divided by its fatigue damage 'life' thus :

$$\frac{da}{dN} = \frac{d^*}{N_f} \quad (3)$$

Now a small crack can be modelled as a ellipse which lies on the surface of an infinite body subject to a uniform tension stress. The opening displacement of an elliptical crack of length $2a$ in an infinite sheet under a uniaxial tension stress σ are given by the relation (8):

$$\delta = 2(1 + \nu)(1 - 2\nu)\sigma a \left(\frac{\sin\theta}{E} \right) \quad (4)$$

where a represents the half surface crack length and θ is the angle between the point of interest and the major axis of the ellipse.

Since the crack is very small it can be regarded reasonably as a 'line crack'. So when a plastic zone of size r_p is formed at the crack tip, we can define δ as the distance of separation of the crack faces due to notional growth of the crack up to the mid-point of the plastic zone. We can represent this case by considering an equivalent elastic microcrack whose tip is located at the boundary of the plastic zone. It is therefore reasonable to assume, in the (x, y) coordinate system, an approximate equality, $x = (a + r_p)\cos\theta$, so we then find that $\sin\theta = [1 - [(x-a)/(a+r_p)]^2]^{1/2}$. The crack opening displacement along the equivalent crack face in the presence of plastic zone under the plane strain condition can then be expressed as

$$\delta = \frac{2(1+\nu)(1-2\nu)}{E} (a + r_p) \left[1 - \left(\frac{x-a}{a+r_p} \right)^2 \right]^{1/2} \sigma \quad (5)$$

As the result of the first loading cycle, the crack tip blunts to a semi-circular micronotch with radius, d^* , (the size of the process zone). d^* thus scales with plastic zone size during small crack propagation. As the crack approaches a grain boundary the size of the process zone is truncated, (6). The evolution of this process has been already investigated in 7000 series aluminium alloys and provides an analytical solution linking process zone d^* , microstructural dimension ρ^* and the ratio of fully developed plastic zone to crack length r_p/a via σ/σ_y , (7). To estimate the size of process zone, we thus simply satisfy the requirement for strain equilibrium at the boundary between the plastic zone ahead of the crack tip and the elastic region surrounding it. We can then estimate the process zone size as:

$$\frac{d^*}{\rho^*} = \frac{\omega}{2} \left(\frac{r_p}{a} \right) \left(1 + \frac{r_p}{a} \right)^{-0.5} \quad (6)$$

where ω is the maximum triaxiality factor, (8) and $2a$ is the surface crack length. Figure 5 illustrates how these variables are connected.

We assume that the plastic strain in the process zone is large so that the contribution of the elastic strain can be ignored and so $\Delta\epsilon_p \approx \Delta\epsilon_{tot}$. Now the normal strain distribution in the yielded zone ahead of the crack can be expressed along the x axis as:

$$\epsilon = \frac{\eta}{x - a} \quad (x > a) \quad (7)$$

where η is the deformation in the yielded zone.

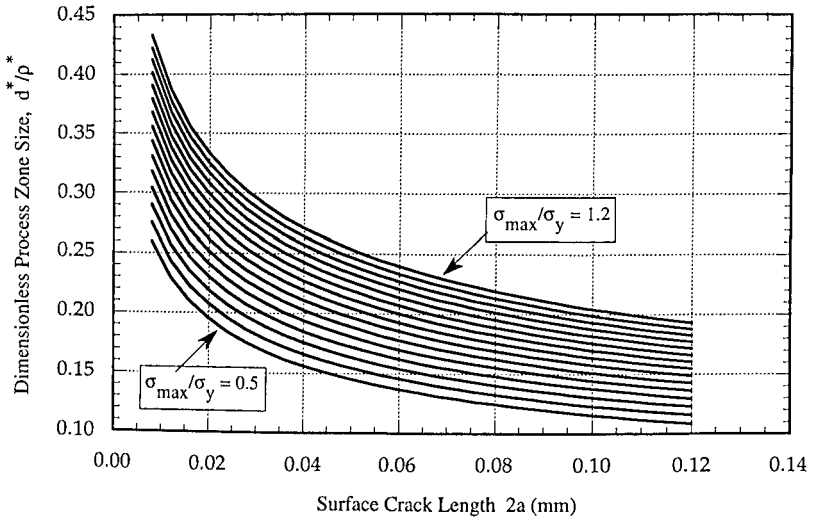


Figure 5 Relationship between, σ_{\max}/σ_y , ρ^* and d^*

In order to avoid a singularity at $x = a$, we assume that the deformation is constant within d^* of the tip of the process zone. If the elementary block of material of length ρ^* is initially elongated by $\delta/2$, we have:

$$\epsilon = \frac{\delta}{2\rho^*\omega} \quad (a \leq x \leq a + d^*) \quad (8)$$

where ω takes a value of 2.57, (9). Continuity requirements between Equations (7) and (8) at $x = a + d^*$ lead to the result that $\eta = (\delta d^*)/(\rho^*\omega)$ which gives

$$\epsilon = \frac{\delta d^*}{2\rho^*\omega (x - a)} \quad \text{for } (a + d^* \leq x \leq a + r_p). \quad (9)$$

Substitution of Equation (5) into Equation(9) then yields:

$$\epsilon = \frac{d^* a (1 + \nu)(1 - 2\nu)}{\rho^* \omega E (x - a)} \left(1 + \frac{r_p}{a}\right) \left[1 - \left(\frac{x/a - 1}{1 + r_p/a}\right)^2\right]^{1/2} \sigma \quad (x > a) \quad (10)$$

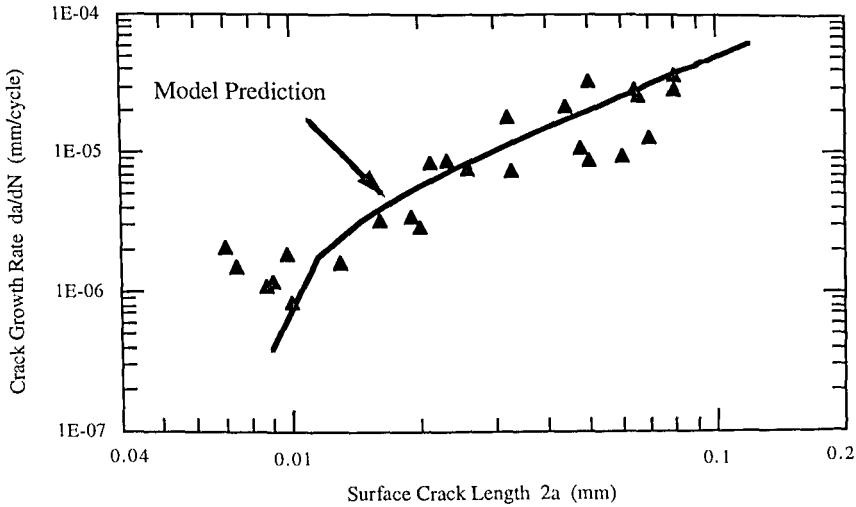


Figure 6 Comparison of Model Prediction with Measured Small Fatigue Crack Data

The frontier between the elastic-plastic zone and its surrounding elastic region is at $x = a + r_p$ and we need the plastic strain at this point which can be evaluated by letting $x = a + d^*$ in Equation 10 giving:

$$\frac{\Delta \epsilon_p}{2} = \frac{(1 + \nu)(1 - 2\nu)}{2\rho^* \omega E} \left(\left(1 + \frac{r_p}{a}\right)^2 - \left(\frac{d^*}{a}\right)^2 \right)^{0.5} \Delta \sigma a. \quad (11)$$

The fatigue life of the process zone can then be deduced from the Coffin-Manson relation thus:

$$\frac{\Delta \epsilon_p}{2} = \left(\frac{\sigma_f' \epsilon_f'}{K'} \right)^{1/(1+n)} (2N_f)^{(b+c)/(1+n')} \quad (12)$$

Since every grain in the alloy is different, the microstructural dimension, ρ^* , should vary randomly. As a first step in modelling this process the average grain size ρ_{ave}^* has been used in our prediction of small crack growth to give :

$$\frac{da}{dN} = 2d^* \left(\left(\frac{K'}{(\sigma_f' - \sigma_m) \epsilon_f'} \right)^{\frac{1}{1+n'}} \frac{\Delta \epsilon_p}{2} \right)^{-\frac{1+n'}{b+c}} \quad (13)$$

Predictions using equation 13 are presented in Figure 6 where reasonable agreement can be seen with measured small crack growth data. Agreement can be seen to be very good.

Discussion

The model has two main predictions: Firstly, small fatigue crack propagation is predicted to be faster in alloys with large grains because the local growth rate is to a great extent controlled by local grain size. This also implies that if a small crack initiates a large favourable oriented grain, the small crack growth rate will, on average, initially reduce with crack size as this grain will be surrounded by grains that are, on average smaller.

Secondly, crack growth rate is predicted to increase with applied stress level . However, since the local growth rate is also very dependent on local grain size, da/dN is actually controlled by an interaction between local stress effects and local grain size effects. This means that growth rates would show scatter with increasing crack length if actual local grain size is used. The net effect of this is that small cracks often grow with large scatter in their propagation rates and show no clear indication of any stress dependence.

Conclusions

- A predictive small fatigue crack growth model has been developed that uses the concept of a process zone to represent the fully damaged zone ahead of a small crack tip.
- The model relies only on an appropriate physical description of the alloy through its bulk fatigue properties in conjunction with microstructural characteristics.
- Good agreement is found between the models predictions and measured small fatigue crack growth rates.
- The model also explains the origins of scatter, grain size dependence and the relatively weak stress dependence of small fatigue crack growth rates.

References

1. K. Tanaka, Y. Akiniwa, Y. Nakai and R. P. Wei, Engng. Fract. Mech., 24, (1986), 803.
2. A. Navarro and E. R. de los Rios, Phil. Mag., 57, (1988), 15.
3. L. Edwards and Y. H. Zhang, Acta Metall. Mater. 42, (1994) 1423.
4. L. Edwards and J.W. Martin, Strength of Metals and Alloys, ed. R.C. Gifkins, (Pergamon Press, 1992), 875.
5. P. J. E. Forsyth, Int. J. Fatigue 5, (1983), 3.
6. Y. H. Zhang and L. Edwards, Scripta Metallurgica, (1992), 1901.
7. L. Edwards and Y. H. Zhang, Acta Metall. Mater. 42, (1994) 1413.
8. I. Mushkhelishvili, Some Basic Problems Of Mathematical Theory Of Elasticity. (Noordhoff, Leiden, 1953)
9. R. Hill The Mathematical Theory Of Plasticity., (Oxford University Press, 1950), 258.